Scientific Research Publishing

Materials Sciences and Applications, 2025, 16(5), 252-268
https://www.scirp.org/journal/msa
ISSN Online: 2153-1188
ISSN Print: 2153-117X

Effect of Al on Zn and Mg on Zn-Al as Pb Free Solder Alloy

Safayet Rafid[1], Suraya Sabrin Soshi[1], Al Fahad Ahmed[2], Md. Abdul Gafur[3]

[1]Department of Mechanical Engineering, Ahsanullah University of Engineering and Technology, Dhaka, Bangladesh
[2]Department of Naval Architecture and Ocean Engineering, Bremen University of Applied Sciences, Bremen, Gemany
[3]Bangladesh Council of Scientific and Industrial Research, Dhaka, Bangladesh
Email: d_r_magafur@yahoo.com

How to cite this paper: Rafid, S., Soshi, S.S., Ahmed, A.F. and Gafur, M.A. (2025) Effect of Al on Zn and Mg on Zn-Al as Pb Free Solder Alloy. *Materials Sciences and Applications*, **16**, 252-268.
https://doi.org/10.4236/msa.2025.165015

Received: September 18, 2024
Accepted: May 24, 2025
Published: May 27, 2025

Abstract

The Zn-Al alloy has garnered immense attention in both fundamental and applied research. In this research, the bulk solder properties of Zn-xAl and Zn-5Al-xMg (x = 4, 5 and 6) systems were explored systematically and compositional, thermal, microstructural, mechanical, and electrical characteristics of these alloys are examined and contrasted appropriately. Differential Thermal Analysis (DTA) revealed that the addition of Al in Zn caused the reduction of the melting temperature of Zn from 419˚C to 376.3˚C and Mg in Zn-5Al caused reduction of the melting temperature of Zn-5Al from 376.3˚C to 343.7˚C, respectively. Microstructures of Zn-xAl alloys with different percentages of Al, exactly resembles to the Zn-Al binary phase diagram. When increasing the amount of Mg up to 6 wt% in Zn-5Al alloy, $MgZn_2$ phase increases gradually and consequently lamellar matrix decreased. Al and Mg addition in Zn and Zn-5Al alloy separately caused to increase the tensile strength of Zn and Zn-5Al alloy. Zn-6Al alloy exhibited the highest tensile strength and fracture strain. Aluminum (Al) is often added to zinc (Zn) alloys to enhance their mechanical properties, including hardness. Also, Mg addition in Zn-5Al caused to gradually increase the hardness of Zn-5Al alloy. With increasing the amount of Al from 4 to 6 wt%, electrical resistivity of the Zn based alloys gradually increased. Since the resistivity of β phase is higher than α phase, electrical resistivity of Zn-5Al-xMg alloys were also higher than Zn-5Al alloy. The lowest resistivity of Zn-5Al-xMg system was found to be 8.329 μΩ·cm for Zn-5Al-5Mg alloy.

Keywords

Tensile Strength, DTA, Solder Alloy, Hardness

1. Introduction

Electronic solder is the prime material used for the interconnections between chip and package or between packaged IC circuit board (PCB). Not only does solder make electrical connections, it is also used to provide mechanical, thermal connections between the components and it's supporting of the printed circuit board. Tin-lead solder has been the most commonly used solder alloy in electronic devices. Pb-Sn alloys with the compositions of 5 - 15 wt% Sn-Pb, which have a melting point in the range of 240 - 310˚C are characterized to be used as solder materials at high temperature [1].

The discovery of microelectronic devices revolutionized the world. However, the performance of these devices is associated with the generation of heat, and their performance is limited due to the thermal degradation of these materials. So far, there are several systems developed to sustain a high temperature and to overcome the thermal degradation. Having an appropriate melting range has been defined by industry as 270 - 350˚C in order to ensure efficient process control [2]. Deposit significant research into lead-free solders and thousands of paper published in recent years, only a small proportion of these specifically relate to high temperature lead-free solders. High-temperature solder alloys are however, a key structural material for various industrial components and assemblies which require a high level of quality and reliability and also to be free from lead. As such, there is need to review the literature to identify the relative strengths and weaknesses of the current generation of lead-free solder alloys suitable for high-temperature applications and identify opportunities for further developments. The current options for high temperature solders, typically designed to withstand temperature between 150 and 200˚C are derived from Pb-Sn, Au-Sn, Au-Ge, Zn-Al, Zn-Sn, Bi-Ag and Sn-Sb alloys, as well as some other alloy systems [3]. Zn-based solders have a lot of prospects due to its competitive price and mechanical properties. The effect of the addition Al, Sn, Cu, Ca, Mg, Cr and Ti is reported so far [2]-[11]. Zn-Sn alloys show a much improved ductility compared to other Zn-based alloys, excellent electrical properties and oxidation resistance at high temperature and humidity [6]-[8]. Though it has eutectic composition of 85 wt% Sn at 199˚C, but it can withstand multiple reflows of up to 260˚C [6].

In these days, Zn-Al alloy are used to join Al structures [4]. Zn-Al phase diagram shows only one eutectic point with a composition of 5 wt% Al at 381˚C [9]. The high oxygen affinity of these alloys with low wettability is the only drawback. Addition of Mg, Sn and in as third element in Zn-Al binary system has been investigated so far [12]-[16]. Zn-Al-Cu solder alloys showed a reasonable electrical resistivity and spreadability making them suitable for electronics applications [12] [13]. Zn-4Al-3Mg-3Ga shows a solids and liquids at 309˚C and 347˚C respectively [15]. Good die-attaching with a very small amount of voids was achieved at 320 ˚C or higher in the die-attaching test with this alloy. However, this alloy had poor workability and low capacity for stress relaxation at room temperature, and thus it is limited in its commercial use. In this work, our aim was to study the bulk

properties of proeutectic, eutectic and hypoeutectic Zn-Al alloys. Yunlong *et al*. worked on the properties(structural, mechanical electrical, chemical etc.) of Zn-Al alloys containing 5% - 25% Al [17].

The present attempt has therefore been taken to investigate the effect of addition of Mg on the structure, thermal and mechanical properties of Zn-based solder alloy.

As the use of solder alloys is join metals on PCB, it is obvious to study the interconnecting properties of the solder alloys to evaluate the performance in a long run. The present study is to analyze the effect of Mg on Zn-Al alloy. Although the addition of Mg increases the electrical resistivity but it also increases the hardness which gives the alloys stability. Besides this, Mg also reduces the melting temperature of alloy which makes the alloy easier to apply. For this purpose initially effect on DTA of the alloy was analyzed. Subsequently the behavior of the alloys' microstructure and micro-hardness were also observed after addition of Mg. Sequentially the tensile test of the alloy having Mg was examined. Finally how electrical resistivity of the alloy changes with combination of Mg was observed. The research focuses on developing high-temperature lead-free solder alloys, which is crucial for advancing electronic materials and ensuring environmental safety. The study provides detailed insights into the effects of Mg addition on the thermal, mechanical, and electrical properties of Zn-Al alloys, which has not been extensively covered in previous literature. The focus on lead-free solder alloys directly addresses current environmental regulations and industrial requirements for safer materials.

2. Experimental Works

Materials and Fabrication Process

Materials used in the research were collected from local market. They were commercially available pure Zn (99.99%), Al (99.99%), and Mg (99.99%). In this research three Zn-xAl, x = 4, 5, 6 alloys and (100-y)(Zn-5Al)·yMg, y = 4, 5, 6 were cast. For Zn-Al-Mg alloys Zn and Al ratio was equal to 95:5 wt. The position of the Zn-4Al, Zn-5Al and Zn-6Al alloy is shown in the vertical lines in the binary Zn-Al phase diagram in **Figure 1**.

Here, it is also shown melting temperature of pure Zn is 419˚C and melting temperature of pure Al is 660˚C. The eutectic temperature of Zn-5Al alloy is 382^0C. The eutectic mixture is the $\alpha'+\beta$ phase which is lamellar structure. At 275˚C the alloy shows a eutectoid point where solid-solid transformations begin.

A batch weighing 420 gm was made each time. Depending upon the composition the amount of raw materials for mixing varied as following **Table 1**. Chemical addition is given below in **Table 1**.

The proportionate raw materials were placed into a graphite crucible as per the amount shown in **Table 1**. Starting materials were different for Zn and Al or Zn, Al and Mg. They were melted in a graphite crucible in the resistance heating furnace and temperature was raised to 750˚C. The Mg was added using special tech-

nique. Mg was taken in Aluminum foil and Ar gas was used during addition of Mg. Then the liquid metal was poured in the metal mold to prepare the alloys. The process of casting is show in Figure 2.

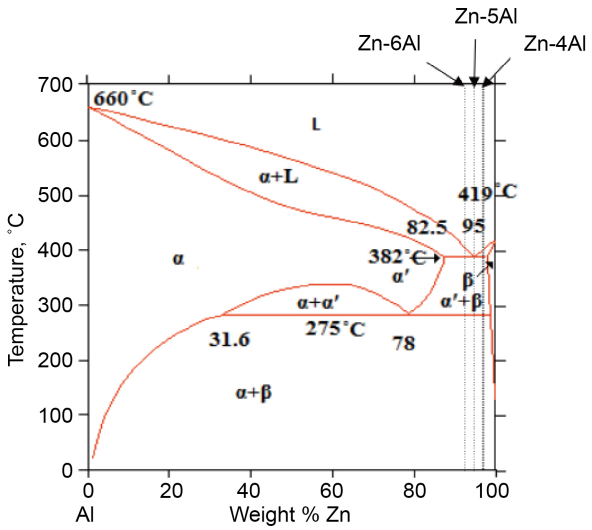

Figure 1. The three Zn-xAl alloys in Zn-Al phase diagram.

Table 1. Chemical composition of solder alloys.

Alloy	Weight of raw materials (gm)			Zn:Al Wt %	Zn-5Al:Mg
	Zn	Al	Mg		
Zn	420	-	-		
Zn-4Al	403.2	16.8	-		
Zn-5Al	399	21	-	-	
Zn-6Al	394.8	25.2	-	-	
Zn-5Al-4Mg	383.04	20.16	16.8	95:5	96:4
Zn-5Al-5Mg	379.05	19.95	21	95:5	95:5
Zn-5Al-6Mg	375.06	19.74	25.2	95:5	94:6

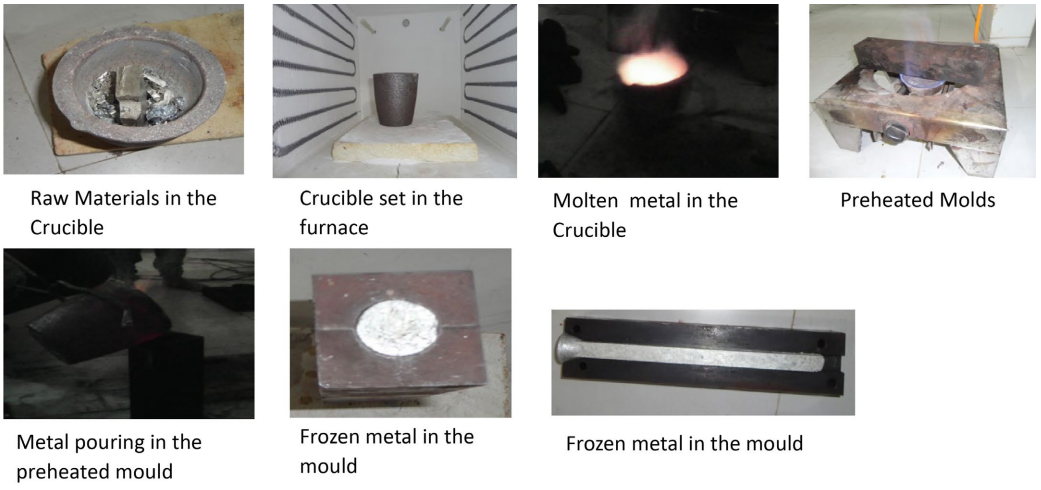

Figure 2. Image showing the steps of casting.

3. Results and Discussion

3.1. Differential Thermal Analysis (DTA) of the Alloys

3.1.1. Melting Behavior of the Zn-xAl (x = 4, 5 and 6) Alloys

Melting temperature, peak temperature and solidification range of these alloys obtained from the DTA test are presented in Table 2. Around 280˚C there is a endothermic small peak for all alloys due to solid-solid phase change ($\alpha \rightarrow \alpha'$). Melting temperature extracted from DTA curves (Figure 3) are presented in Figure 4. It is seen that melting temperature of pure Zn was 419˚C. It is also found that melt starting temperature (solidus temperature) of Zn-4Al, Zn-5Al, Zn-6Al alloys are 376.4˚C, 376.3˚C and 376.5˚C. This is due to the eutectic transformation at 382˚C, show in the Zn-Al phase diagram in Figure 1. The variation might be due to presence of traceable elements. Very similar results were obtained by MM Hasan *et al*. [18].

Table 2. DTA result of Zn and Zn-xAl alloys.

	Peak Temp.; ˚C	Melt starting Temp.; ˚C	Melt ending Temp.; ˚C	Solidification Range Temp.; ˚C
Zn	428.0	419.0	449.70	30.7
Zn-4Al	400.5	376.4	422.4	46.0
Zn-5Al	396.9	376.3	418.2	41.9
Zn-6Al	394.9	376.5	417.0	40.5

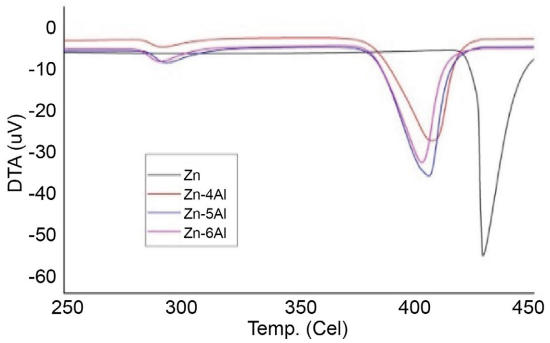

Figure 3. DTA curves of Zn and Zn-xAl alloy.

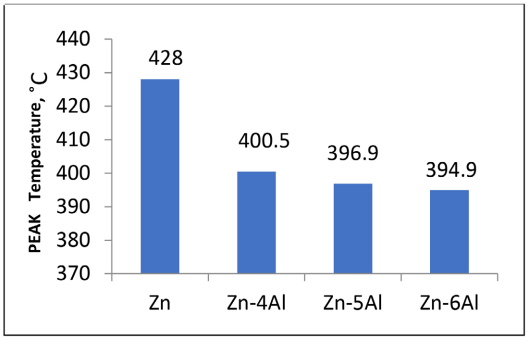

Figure 4. The effect of Al addition on the peak temperature of Zn.

Solidification range of the alloy extracted from Figure 3 is shown in Figure 5. It is seen that the solidification range of pro-eutectic Zn-4Al alloy was 46˚C and the solidification range of the hypereutectic Zn-6Al alloy was 40.5˚C. The solidification range of the eutectic composition alloy Zn-5Al was found 41.9˚C. The eutectoid transformation is identified in the DTA curves of the Zn-xAl alloys. Although the eutectoid transformation in Zn-xAl alloys is observed at 275˚C in Zn-Al binary phase diagram, but in this research it is found in nearly 280˚C. The difference in heating rate and the change in the atmospheric condition is the reason for the difference in eutectoid transformation temperature.

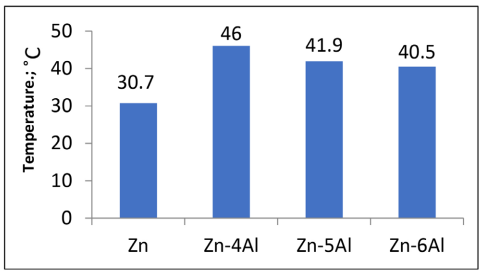

Figure 5. Showing the transformation range of Zn-xAl alloys.

Table 3. DTA result of Zn-5Al, Zn-5Al-4Mg, Zn-5Al-5Mg and Zn-5Al-6Al alloys.

Alloys	Melt starting Temp.; ˚C	Melt ending Temp.; ˚C
Zn-5Al	376.3	418.2
Zn-5Al-4Mg	343.2	385.5
Zn-5Al-5Mg	343.9	383.5
Zn-5Al-6Mg	343.7	384.1

3.1.2. Melting Behavior of Zn-5Al-xMg (x = 4, 5 and 6) Alloys

DTA curves of these alloys obtained from the DTA test (EXSTAR 6000 TG/DTA 6300, Seiko Instrument, Japan) are presented in Figure 6. Table 3 shows the melting staring and ending temperature. Melting temperature, peak temperature and solidification range of the alloy extracted from Figure 6 are shown in Table 4, Figure 7 and Figure 8, respectively. It is seen from Table 4 that addition of Mg up to 6 wt% causes to reduce the start of melting of the Zn-5Al alloys from 376.3˚C to 343.2˚C. The eutectic temperature of Zn-5Al is 382˚C (Figure 1). Also from Figure 7 it is found that the minimum peak temperature of Zn-5Al-6Mg alloy is 352.2˚C. With addition of Mg the peak temperature is reduced from 396.9˚C to 352.2˚C.

Solidification range of the alloys extracted from Figure 6 is shown in Figure 7. It is seen that the solidification range of Zn-5Al-4Mg alloy was 42.3˚C and Zn-5Al-6Mg alloy was 40.4˚C. The minimum solidification range of 39.6˚C found for the Zn-5Al-5Mg alloy. The eutectoid transformation is identified by small endothermic peak in the DTA curves of the Zn-5Al-xMg alloys shown in Figure 6. The

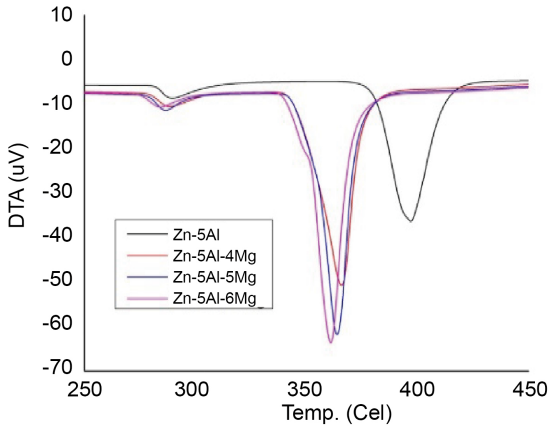

Figure 6. DTA curves of Zn-5Al and Zn-5Al-xMg alloys.

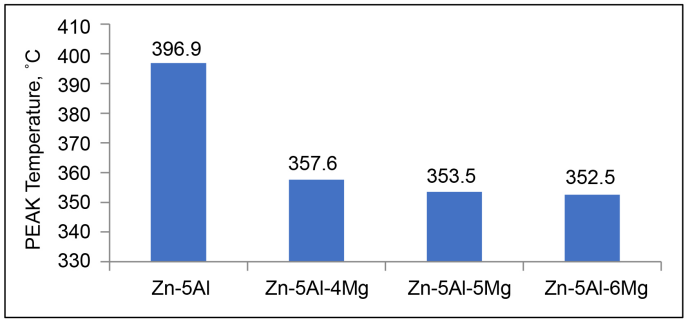

Figure 7. The effect of Mg addition on the peak temperature of Zn-5Al on heating.

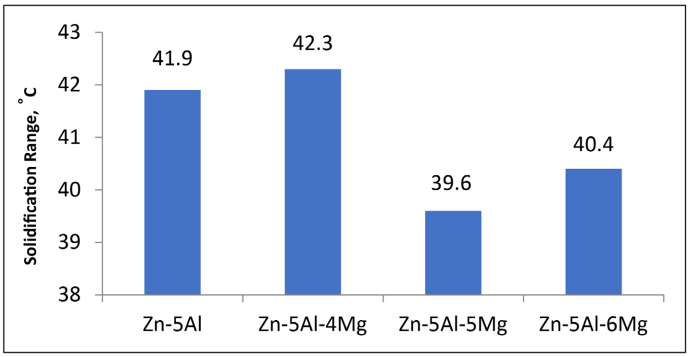

Figure 8. The effect of Mg addition on the transformation range of Zn-5Al-xMg alloys.

Table 4. DTA result of Zn-5Al, Zn-5Al-4Mg, Zn-5Al-5Mg and Zn-5Al-6Al alloys.

Alloys	Melt starting Temp.; ˚C	Melt ending Temp.; ˚C
Zn-5Al	376.3	418.2
Zn-5Al-4Mg	343.2	385.5
Zn-5Al-5Mg	343.9	383.5
Zn-5Al-6Mg	343.7	384.1

eutectoid transformation in Zn-5Al alloy is observed at 275˚C in the Zn-Al binary phase diagram. For the addition of Mg in Zn-5Al binary alloy in this research it is found in nearly 280˚C, also the difference in heating rate and the change in the atmospheric condition is the reason for the difference in the eutectoid transformation temperature.

3.2. Microstructural Characterization of Alloys

Ingots of solder alloys were cast in metal mold. At first commercially available Zn was cast. Then Zn-Al alloy with three different percentage of Al containing 4, 5 and 6 wt% Al alloys were cast. To study the effect of Mg on Zn-5Al alloy was also studied by casting Zn-5Al-4Mg, Zn-5Al-5Mg and Zn-5Al-6Mg alloys.

3.2.1. Microstructure of Zn

Microstructure analysis of the metallographically prepared Zn-xAl alloys is carried out in an optical microscope (MMT-500T, MTI Corporation, USA) in order to know the distribution of the different phases at a magnification of 200×. Figure 9 shows the optical micrograph of Zn alloy. In the microstructure of the pure Zn, only homogenous grains of Zn are seen. The pores are also observed in the microstructure. The pores are seen for some impurities to remain in the Zn alloy when it was cast. Pure Zn grains were directly solidified from the liquid (L → Pure Zn Grains).

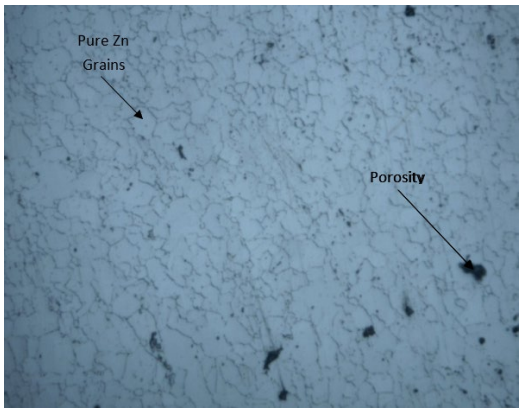

Figure 9. Optical micrograph of Pure Zn at 500× showing pure Zn grains.

3.2.2. Microstructure of Zn-xAl (x = 4, 5 and 6) Alloys

Figure 10 shows the microstructures of different Zn-xAl solder alloys under the same optical microscope.

Figure 10(a) shows microstructure of Zn-4Al alloy showing the presence of proeutectic β in a lamellar (eutectic) matrix. Hundred percentage lamellar structures are seen in the microstructure of the Zn-5Al alloy in Figure 10(b). Zn-6Al alloy shows the dark proeutectic α in the matrix of lamellar structure in Figure 10(c). Here a continuous outer layer of bright β phase is seen at the surroundings of α.

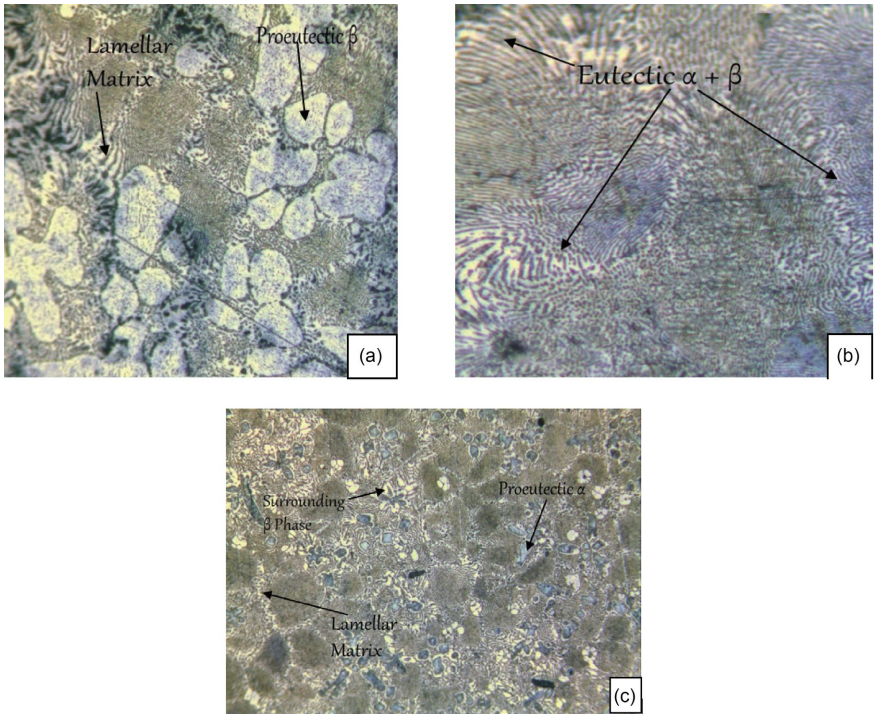

Figure 10. Optical micrograph of (a) Zn-4Al, (b) Zn-5Al and (c) Zn-6Al alloys at 200× showing β, and α phase.

The solidification of Zn-4Al alloy was started with the nucleation of the proeutectic β and completed with the eutectic transformation of ($\alpha' + \beta$). A eutectoid transformation of α' to ($\alpha + \beta$) took place at 282˚C. The eutectoid phase ($\alpha + \beta$) along with the proeutectic phase β is seen in the final microstructure of as cast Zn-4Al alloy in **Figure 10(a)**. The transformation order can be shown as below:

L → Proeutectic β + L_1 → Proeutectic β + Eutectic ($\alpha' + \beta$) → Proeutectic β + Eutectic (Eutectoid ($\alpha + \beta$) + Eutectic β).

Figure 10(b) depicts the presence of lamellar structure solely. The eutectic alloy Zn-5Al is solidified directly to the lamellar structure of ($\alpha' + \beta$). A solid-solid transformation of α' to eutectoid ($\alpha + \beta$) occurs at low temperature. The transformation order of Zn-5Al alloy is shown in below:

L → Eutectic ($\alpha' + \beta$) → (Eutectoid ($\alpha + \beta$) + Eutectic β)

Figure 10(c) is the microstructure of hypereutectic Zn-6Al alloy. Here, the presence of pro-eutectic α phase in a mixture of lamellar matrix is observed. Moreover, α phase is seemed to be surrounded continuously by a thin layer of β phase due to the drift of the Al atoms towards α phase. The transformation order of Zn-6Al alloy is shown in below:

L → Proeutectic α + L_1 → Proeutectic α + Eutectic ($\alpha' + \beta$) → Proeutectic α + (Eutectoid ($\alpha + \beta$) + Eutectic β)

3.2.3. Microstructure of Zn-5Al-xMg (x = 4, 5 and 6) Alloys

Figure 11 shows the optical micrograph of Zn-5Al-xMg alloys at magnification of 200×. From previous discussion, we have seen that Zn-5Al alloy has solely lamel-

lar structure. So, with addition of Mg with Zn-5Al, a new phase appeared, which is $MgZn_2$. This phase dominates at higher amount of Mg. Figure 11(a) shows the microstructure of Zn-5Al-4Mg alloy. This microstructure proves the presence of $MgZn_2$ phase. And with increasing the amount of Mg (*i.e.* Zn-5Al-5Mg and Zn-5Al-6Mg), $MgZn_2$ phases also further increases.

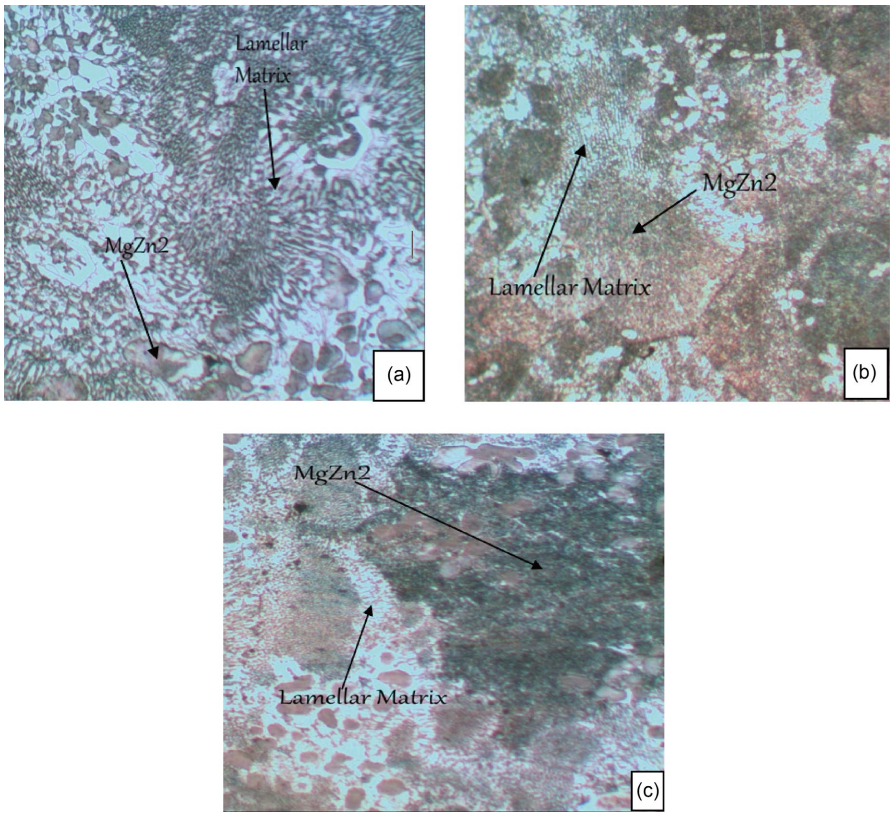

Figure 11. Showing the optical micrograph of (a) Zn-5Al-4Mg, (b) (Zn-5Al-5Mg) Zn-5Al-6Mg.

3.3. Mechanical Properties

Tensile Properties

1) Tensile Testing of Zn-xAl (x = 4, 5 and 6) Alloys

The stress-strain curves of Zn, Zn-4Al, Zn-5Zn and Zn-6Al alloys are given in Figure 12. Through at least three tensile samples of each category were tested, but in the figure only the representative data of the samples is in consideration.

Ultimate Tensile Strength (UTS) and fracture strain of the Zn and Zn-xAl alloys are shown in Figure 13. From the figure, it is clear that the Al addition in Zn causes to increase both the Ultimate Tensile Strength (UTS) and fracture strain value. It also found that, among the Zn-xAl alloys, the highest Ultimate Tensile Strength (UTS) (189.69 MPa) and fracture strain (11.34%) are found for the Zn-6Al alloys. Very similar UTS was found for Zn-7Al (≈180 MPa) by Annali Pola *et al.* [19]. With the increase of Al, the microstructure changes to the lamellar matrix containing β phase resulting in increase of UTS.

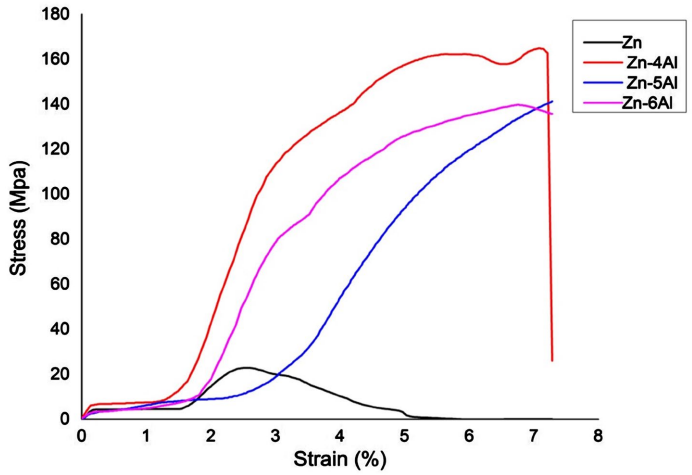

Figure 12. Typical stress-strain curve of Zn, Zn-4Al, Zn-5Zn and Zn-6Al alloys.

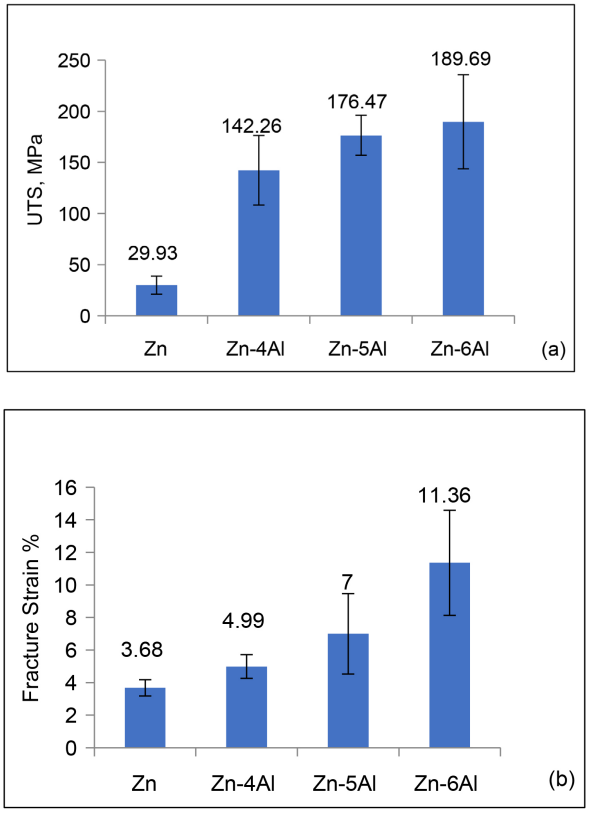

Figure 13. (a) Ultimate Tensile Strength (UTS) and (b) fracture strain of Zn and Zn-xAl Alloys.

2) Tensile Testing of Zn-5Al-xMg (x = 4, 5 and 6) Alloys

In below the stress-strain plot of the representative of Zn-5Al, Zn-5Al-4Mg, Zn-5Al-5Mg & Zn-5Al-6Mg is shown for general comparison (**Figure 14**)

Ultimate Tensile Strength (UTS) and fracture strain of the Zn-5Al Zn-5Zn-4Mg, Zn-5Zn-5Mg and Zn-5Al-6Mg alloys are **Figure 15(a)** and **Figure 15(b)**. It

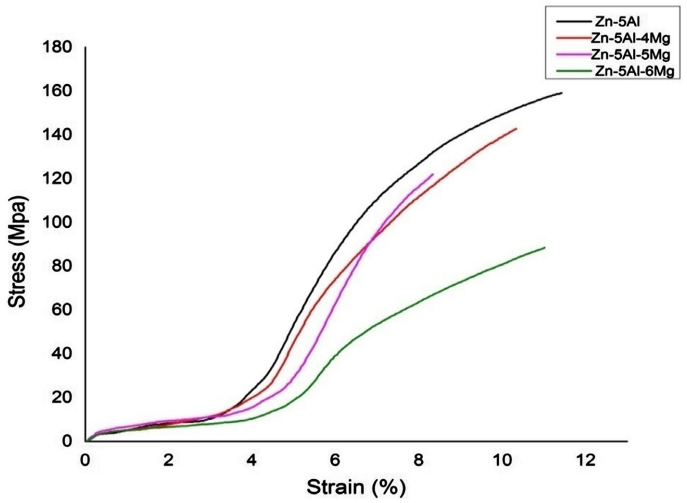

Figure 14. Typical stress-strain curve of Zn-5Al, Zn-5Zn-4Mg, Zn-5Zn-5Mg and Zn-5Al-6Mg alloys.

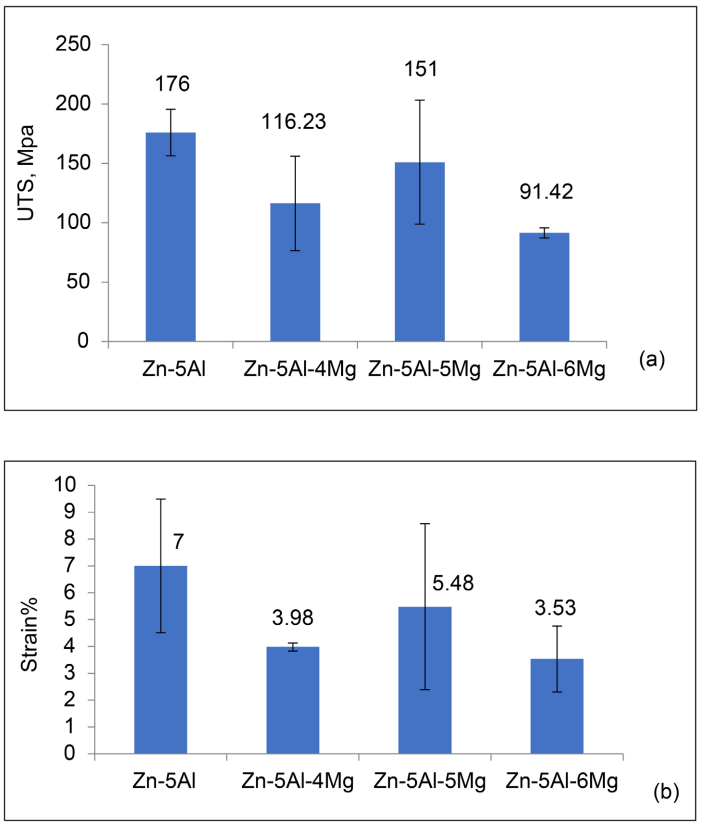

Figure 15. (a) Ultimate Tensile Strength (UTS) and (b) fracture strain of Zn-5Al and Zn-5Al-xMg Alloys.

is found that Zn-5Al alloy has the highest Ultimate Tensile Strength (UTS) and fracture strain value compared to the other Zn-5Al-xMg alloys. Between the Zn-5Al-xMg alloys, the fracture strain of the Zn-5Al-5Mg alloy is the maximum and the lowest fracture strain is found for the Zn-5Al-6Mg alloy. With the increase of

Mg, the lamellar matrix microstructure changes to containing $MgZn_2$ intermetallic compounds phase resulting decrease UTS. As the $MgZn_2$ is brittle phase, with the increases of Mg addition the $MgZn_2$ phase increases resulting in decrease of strength and strain (Figure 15(a), Figure 15(b)).

3.4. Vickers Microhardness

3.4.1. Vickers Microhardness of Zn-xAl (x = 4, 5 and 6) Alloys

Vickers microhardness testing of the samples is carried out to compare the mechanical properties of alloys at five different loads for 5 of indentation time. Figure 16 shows that the hardness of the Zn-xAl alloys is higher than the Zn alloys. Hardness of the Zn-xAl alloys increased with increasing the Al content in Zn up to 6 wt %. With the increase of Al, the microstructure changes to the lamellar matrix containing β phase resulting increase UTS.

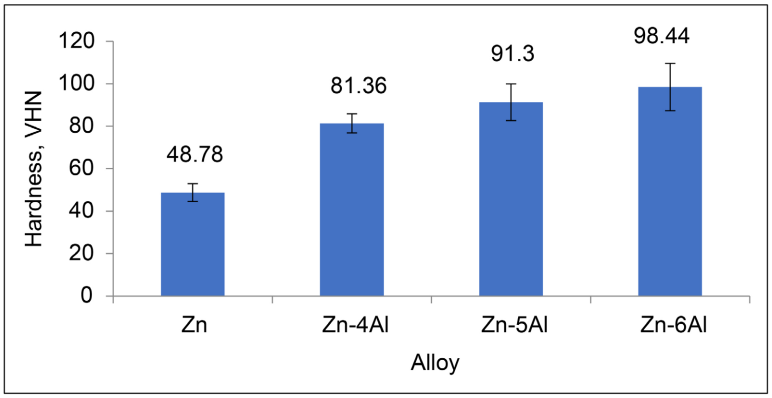

Figure 16. Vickers microhardness of the Zn-xAl alloys.

3.4.2. Vickers Microhardness of Zn-5Al-xMg (x = 4, 5 and 6) Alloys

Figure 17 shows the effect of Mg addition Hardness of the Zn-5Al and Zn-5Al-xMg alloys. It is found the hardness of the Zn-5Al-Mg alloys is higher than the Zn-5Al alloy. Among the Zn-5Al-xMg alloys Zn-5Al-4Mg alloy has the lowest hardness of 158.4VHN and Zn-5Al-6Mg alloy has the highest of 195.41 VHN. With the increase of Mg, the lamellar matrix microstructure changes to containing $MgZn_2$ intermetallic compounds phase. As the $MgZn_2$ is brittle phase, with the increases of Mg addition the $MgZn_2$ phase increases resulting in continuous increase in hardness. It is very similar to hypereutectoid steel, where hardness increases continuously with the increase of carbide phase.

3.5. Electrical Resistivity Analysis

3.5.1. Electrical Resistivity of Zn-xAl (x = 4, 5 and 6) Alloys

The effect of the Al addition on electrical resistivity is shown Figure 18. It is observed that the electrical resistivity of the Zn-4Al and Zn alloys are same. On the other hand, the resistivity of 5 wt% Al added alloy is higher compared to the Zn alloy but 6 wt% Al added alloy is lower compared to the Zn alloy. The variations obtained are not significant.

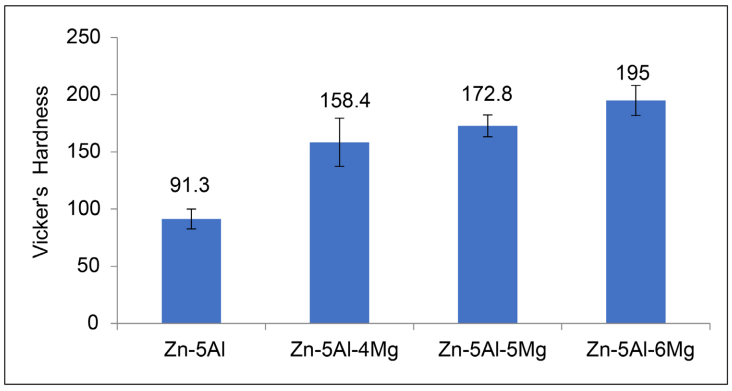

Figure 17. Vickers microhardness of the Zn-5Al and Zn-5Al-xMg alloys.

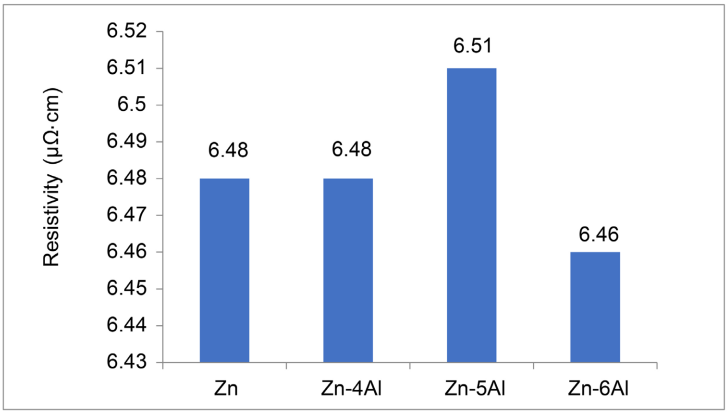

Figure 18. Showing the electrical resistivity of Zn-xAl binary alloys.

3.5.2. Electrical Resistivity of Zn-5Al-xMg (x = 4, 5 and 6) Alloys

Figure 19 shows the effect Mg addition on the resistivity of the Zn-5Al-aAlloys. It is observed that the electrical resistivity of Zn-5Al-xMg alloys is higher compared to the Zn-5Al alloy. Among the Zn-5Al-xMg alloys, Zn-5Al-6Mg has the maximum resistivity value of 11.05 μΩ·cm. Zn-5Al is lamellar eutectic phase, which means continuous sound phase. But with the increase of Mg, $MgZn_2$ phase inclusion was found in the eutectic phase resulting in disruption the structure. As a result the resistivity increases continuously.

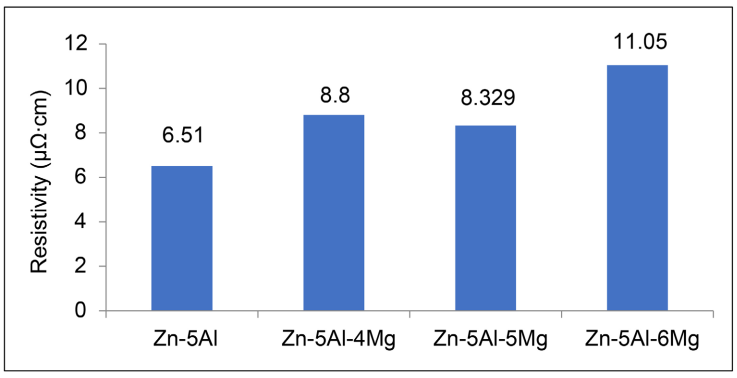

Figure 19. The electrical resistivity of Zn-5Al and Zn-5Al-xAl alloys.

4. Conclusions

In summary, the primary focus of this study was on the thermal, microstructural, mechanical, and electrical properties of the solder alloys Zn-xAl and Zn-5Al-xMg (x = 4, 5, 6). The addition of magnesium in Zn-5Al and aluminium in Zn decreased the melting temperatures, improving the alloys' suitability for soldering. In particular, the inclusion of Al lowered Zn's melting temperature from 419˚C to 376.3˚C, while the addition of Mg further lowered Zn-5Al alloys' melting point to 343.2˚C. Zn-xAl alloys' microstructures also display the binary phase diagram. Additionally, we noticed that the alloys' mechanical qualities improved with the addition of Al and Mg. The maximum ultimate tensile strength (189.69 MPa) and fracture strain (11.34%) were found in Zn-6Al. The Mg-added alloy with the highest fracture strain is Zn-5Al-5Mg. Hardness increase with Mg concentration and peaked for Zn-5Al-6Mg at 195.41 VHN. Zn alloys' electrical resistivity was not affected by the addition of Al, whereas Zn-5Al's resistivity increased when magnesium was added. The Zn-5Al-6Mg alloy had the highest resistivity (11.05 μΩ·cm) that was measured. Overall, this study shows that adding Mg to Zn-5Al solder alloys increases their electrical resistivity. With the increase of Al in Zn, UTS, Strain, and hardness increases, while Mg addition in Zn-5Al alloy hardness increased but strength and strain decreases. These results help to create more dependable electronic connections by offering a foundation for choosing the best Zn-Al-Mg solder compositions for high-temperature lead-free soldering applications.

1) **Mechanical Properties**: Al additions improved the mechanical properties of the alloys. Zn-6Al exhibited the highest ultimate tensile strength (189.69 MPa) and fracture strain (11.34%). However, Addition of Mg in Zn-5Al alloy, decreased in tensile strength and strain, while hardness increased. Zn-5Al-5Mg showing the highest fracture strain among Mg-added alloys. Maximum hardness 195.41 VHN for Zn-5Al-6Mg.

2) **Electrical Conductivity**: Al addition does affect the electrical conductivity of Zn alloys, but Mg addition in Zn-5Al led to higher resistivity. The highest resistivity (11.05 μΩ·cm) was observed in the Zn-5Al-6Mg alloy.

Overall, this study highlights that the addition of Mg changes the mechanical strength, hardness, and processability of Zn-based solder alloys while increasing electrical resistivity. These findings provide a basis for selecting optimal Zn-Al-Mg solder compositions for high-temperature lead-free soldering applications, contributing to the development of more reliable electronic interconnections.

Conflicts of Interest

The authors declare no conflicts of interest regarding the publication of this paper.

References

[1] Bader, W.G. (1975) Lead Alloys for High Temperature Soldering of Magnet Wire. *Journal of Welding*, **54**, 370-375.

[2] Takaku, Y., Felicia, L., Ohnuma, I., Kainuma, R. and Ishida, K. (2007) Interfacial Reaction between Cu Substrates and Zn-Al Base High-Temperature Pb-Free Solders. *Journal of Electronic Materials*, **37**, 314-323. https://doi.org/10.1007/s11664-007-0344-9

[3] Yamada, Y., Takaku, Y., Yagi, Y., Nakagawa, I., Atsumi, T., Shirai, M., *et al*. (2007) Reliability of Wire-Bonding and Solder Joint for High Temperature Operation of Power Semiconductor Device. *Microelectronics Reliability*, **47**, 2147-2151. https://doi.org/10.1016/j.microrel.2007.07.102

[4] Gueijman, S.F., Schvezov, C.E. and Ares, A.E. (2012) Tracking Interphases in Directionally Solidified Zn-Al Binary Alloys. *Materials Performance and Characterization*, **1**, Article 20120017. https://doi.org/10.1520/mpc20120017

[5] Nagaoka, T., Morisada, Y., Fukusumi, M. and Takemoto, T. (2011) Selection of Soldering Temperature for Ultrasonic-Assisted Soldering of 5056 Aluminum Alloy Using Zn-Al System Solders. *Journal of Materials Processing Technology*, **211**, 1534-1539. https://doi.org/10.1016/j.jmatprotec.2011.04.004

[6] Kim, Y.M., Oh, C., Roh, H. and Kim, Y. (2009) A New Cu-Zn Solder Wetting Layer for Improved Impact Reliability. 2009 59*th Electronic Components and Technology Conference*, San Diego, 26-29 May 2009, 1008-1013. https://doi.org/10.1109/ectc.2009.5074135

[7] Lee, J., Kim, K., Suganuma, K., Takenaka, J. and Hagio, K. (2005) Interfacial Properties of Zn-Sn Alloys as High Temperature Lead-Free Solder on Cu Substrate. *Materials Transactions*, **46**, 2413-2418. https://doi.org/10.2320/matertrans.46.2413

[8] Kim, S., Kim, K., Kim, S. and Suganuma, K. (2008) Interfacial Reaction and Die Attach Properties of Zn-Sn High-Temperature Solders. *Journal of Electronic Materials*, **38**, 266-272. https://doi.org/10.1007/s11664-008-0550-0

[9] Takahashi, T., Komatsu, S., Nishikawa, H. and Takemoto, T. (2010) Improvement of High-Temperature Performance of Zn-Sn Solder Joint. *Journal of Electronic Materials*, **39**, 1241-1247. https://doi.org/10.1007/s11664-010-1233-1

[10] Osório, W.R., Freire, C.M. and Garcia, A. (2005) The Effect of the Dendritic Microstructure on the Corrosion Resistance of Zn-Al Alloys. *Journal of Alloys and Compounds*, **397**, 179-191. https://doi.org/10.1016/j.jallcom.2005.01.035

[11] Park, S.W., Sugahara, T., Kim, K.S. and Suganuma, K. (2012) Enhanced Ductility and Oxidation Resistance of Zn through the Addition of Minor Elements for Use in Wide-Gap Semiconductor Die-Bonding Materials. *Journal of Alloys and Compounds*, **542**, 236-240. https://doi.org/10.1016/j.jallcom.2012.07.040

[12] Kang, N., Na, H.S., Kim, S.J. and Kang, C.Y. (2009) Alloy Design of Zn-Al-Cu Solder for Ultra High Temperatures. *Journal of Alloys and Compounds*, **467**, 246-250. https://doi.org/10.1016/j.jallcom.2007.12.048

[13] Kim, S., Kim, K., Kim, S., Kang, C. and Suganuma, K. (2008) Characteristics of Zn-Al-Cu Alloys for High Temperature Solder Application. *Materials Transactions*, **49**, 1531-1536. https://doi.org/10.2320/matertrans.mf200809

[14] Li, L., Liu, Y., Gao, H. and Gao, Z. (2012) Phase Formation Sequence of High-Temperature Zn-4Al-3Mg Solder. *Journal of Materials Science: Materials in Electronics*, **24**, 336-344. https://doi.org/10.1007/s10854-012-0751-4

[15] Haque, A., Lim, B.H., Haseeb, A.S.M.A. and Masjuki, H.H. (2011) Die Attach Properties of Zn-Al-Mg-Ga Based High-Temperature Lead-Free Solder on Cu Leadframe. *Journal of Materials Science: Materials in Electronics*, **23**, 115-123. https://doi.org/10.1007/s10854-011-0511-x

[16] Gancarz, T., Pstruś, J., Fima, P. and Mosińska, S. (2012) Thermal Properties and Wetting Behavior of High Temperature Zn-Al-In Solders. *Journal of Materials Engineering and Performance*, **21**, 599-605. https://doi.org/10.1007/s11665-012-0146-y

[17] Zhai, Y., Wang, T., Liu, M., Zhou, N. and Li, X. (2024) Effect of Al Content on the Microstructure and Properties of Zn-Al Solder Alloys. *Metals*, **14**, Article 689. https://doi.org/10.3390/met14060689

[18] Hasan, M.M., Sharif, A. and Gafur, M.A. (2019) Characteristics of Eutectic and Near-Eutectic Zn-Al Alloys as High-Temperature Lead-Free Solders. *Journal of Materials Science*: *Materials in Electronics*, **31**, 1691-1702. https://doi.org/10.1007/s10854-019-02687-x

[19] Pola, A., Tocci, M. and Goodwin, F.E. (2020) Review of Microstructures and Properties of Zinc Alloys. *Metals*, **10**, Article 253. https://doi.org/10.3390/met10020253